Landmarks in Earth Reinforcement, Ochiai et al. (eds),
© 2001 Swets & Zeitlinger, ISBN 90 2651 863 3

Irregular shaking table tests on seismic stability of reinforced-soil retaining walls

Kenji Watanabe, Masaru Tateyama & Kenichi Kojima
Railway Technical Research Institute, Japan

Junichi Koseki
Institute of Industrial Science, University of Tokyo, Japan

ABSTRACT: In order to establish practical design procedures to evaluate seismic stability of different types of retaining walls against high seismic loads, a series of shaking table tests with irregular wave were conducted on retaining wall models consisting of six different types. In these tests, reinforced-soil retaining wall models with a rigid full-height facing exhibited ductile behavior compared to conventional type retaining wall model such as gravity-type, leaning-type and cantilever type ones. This is because when the conventional type wall started to tilt, the subsoil reaction force at the toe of wall suddenly decreased due to loss of bearing capacity. On the other hand, under similar conditions, tensile force in the reinforcement of reinforced-soil walls could be mobilized effectively to resist against the overturning.

1 INTRODUCTION

In recent years, there have been several damages on retaining walls(RWs) due to large earthquake. For example, the Hyogoken-Nanbu earthquake of January 17, 1995, caused serious damages to conventional masonry and concrete gravity-type RWs for railway embankments. On the other hand, the reinforced-soil RWs exhibited ductile behavior and did not reach to critical failure as reported by Tatsuoka et al. (1996). The main loads acting on the retaining wall during earthquake are inertia force, subsoil reaction, seismic earth pressure and tensile force in the reinforcement as schematically shown in Figure I. The subsoil reaction force and the seismic earth pressure are affected by the dynamic interaction between the wall and the soil, of which the detail mechanisms have not been understood well. Further, for the reinforced-soil wall, the interaction between the soil and the reinforcement, and the seismic behavior of the reinforced and unreinforced zones of the backfill have not been understood in detail, either. For these reasons mentioned above, it is diffi-cult to predict the seismic behavior of the RWs rationally.

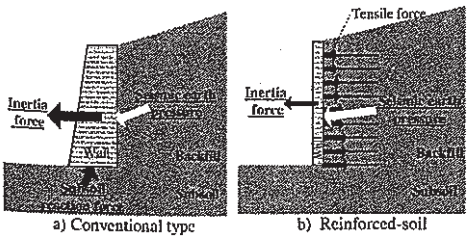

Figure 1. The main forces acting on the wall during earthquake.

It should be also noted that, in the current aseismic design procedures based on the pseudo-static approach, the different extents of ductility and seismic performances of different types of retaining walls are not taken into account properly.

In this study, therefore, a series of relatively small-scale model tests was conducted on the different types of RWs to compare their different performances during irregular shaking.

2 TESTING PROCEDURES

2.1 *Model of retaining wall and backfill*

The model tests were conducted by using the shaking table at Railway Technical Research Institute. A rigid soil container (260 cm long, 60 cm wide, and 140cm high) was fixed to this table.

The cross-sections of six different model retaining walls are shown in Figure 2. The models were 600 mm in width (Figure 3). They consists of three conventional RWs (cantilever type, gravity type and leaning type) and three types of reinforced-soil RWs with a full height rigid facing having different arrangements of reinforcement layers (reinforced-soil RWs type 1, type 2 and type 3). The total height of the conventional walls was 530 mm, while that of the reinforced-soil walls was 500 mm. The bottom width at the base of the cantilever and gravity type walls was 230 mm, while it was reduced to 180 mm for the leaning type wall. To adjust the dead load of the gravity and the leaning type walls, extra weights were added nearly at the center of gravity of these walls.

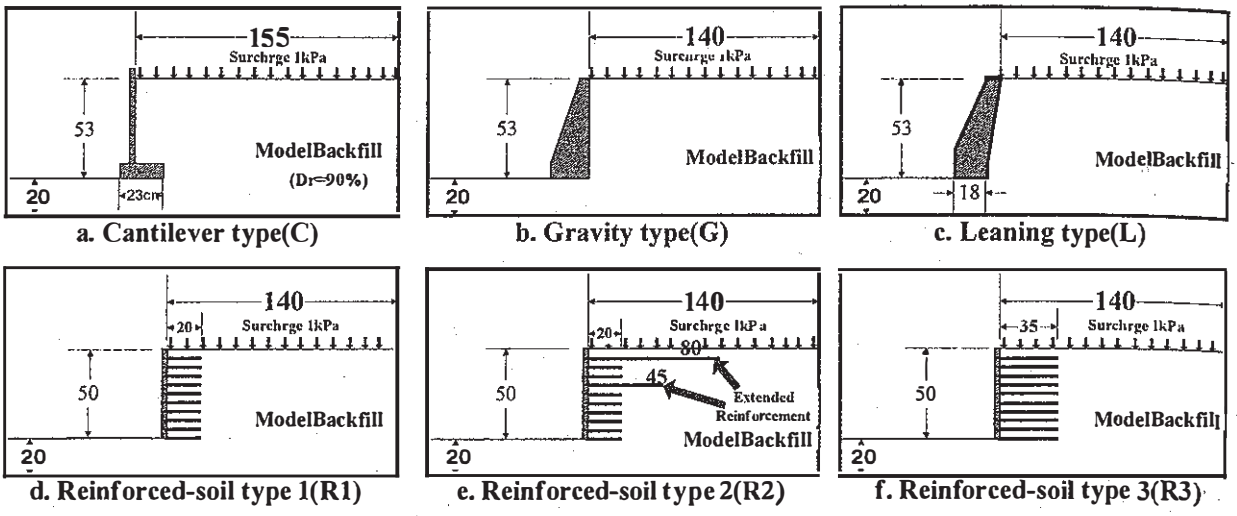

Figure 2. Cross-section of model retaining walls (unit in cm).

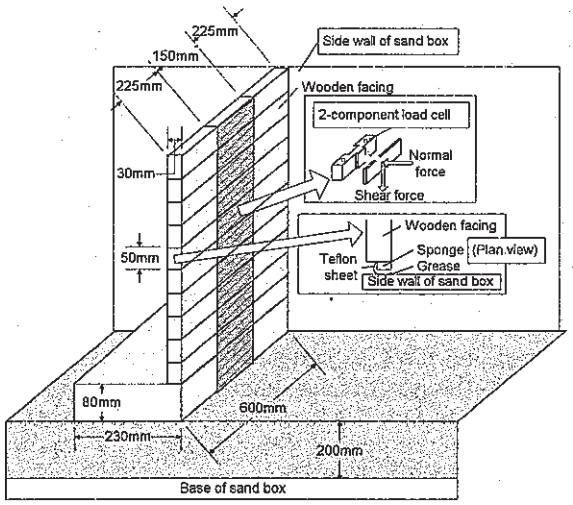

Figure 3. Details of typical wall model (Gravity type).

For the reinforced-soil RW models, a grid of phosphor-bronze strips was used as the model reinforcement. Ten layers of reinforcement strips having a length of 200 mm were horizontally placed in the backfill sand for reinforced-soil wall type1. The length of the top and fourth reinforcement layers was increased to 800 mm and 450 mm, respectively, for the reinforced-soil wall type 2 in order to increase the stability against overturning failure, as is the common practice in Japan. To study into effects of length of the reinforcement layers, the length of all the reinforcement layers was increased to 350 mm for the reinforced-soil wall type 3. Strain gauges were attached to the reinforcement to measure the tensile force.

The subsoil and the backfill layers were made of air-dried Toyoura sand (D_{50}=0.23mm, Gs=2.648, e_{max}=0.977, e_{min}= 0.609). The sand layers were prepared by using a sand hopper with keeping the falling height of sand constant. An average relative density of 90% was achieved by this method.

To observe the deformation and displacement of sand layers, horizontal layers of black-dyed Toyoura sand having a thickness of 10 mm were prepared at a vertical spacing of 50 mm adjacent to the transparent side wall.

The seismic earth pressure acting on the backface of the wall and the subsoil reaction at bottom of base footing were monitored by using two-component load cells which can record both the normal and shear components of earth pressure as shown in Figure 3. The load cells were placed along the center line of the wall surface in order to reduce the effects of the side wall friction of the soil container.

To measure the response of each retaining wall and backfill, a number of displacement transducers and accelerometers were installed. The detail of the model is described in Koseki et al. (1998)

2.2 *Shaking table tests*

Seismic loads were applied by shaking the sand box horizontally with an irregular base acceleration. A strong motion that was recorded as N-S component at Kobe Marine Meteorological Observation Station during the 1995 Hyogoken-Nanbu earthquake was employed as the base acceleration (Figure 4). Its am-

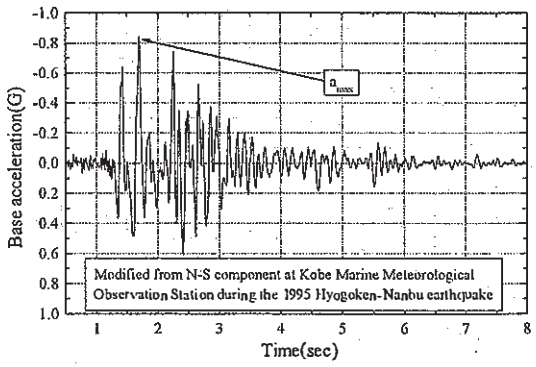

Figure 4. Typical time history of base acceleration.

plitude and time scale were adjusted so that the base acceleration has a prescribed maximum amplitude with a predominant frequency of 5 Hz. Each model was subjected to several shaking steps, where the maximum amplitude of the base acceleration was initially set to 100 gals and increased at an increment of 100 gals. Shaking was terminated when the wall displacement became considerably large.

3 TEST RESULTS AND DISCUSSION

3.1 *Failure pattern of models*

Figure 5 shows the residual displacement of the wall and the residual deformation of the backfill, which were observed at the end of final shaking step.

For all RWs, the major failure pattern of the walls was overturning, which was associated with bearing capacity failure for the cantilever, leaning, and gravity type RWs.

For the reinforced-soil walls, no failure plane was observed at the bottom of the front wedge in the reinforced zone. The front wedge did not behave as rigid, but it suffered simple shear deformation along horizontal planes. This is because the resistance against the formation of failure plane penetrating though the reinforcement was larger than that against the simple shear deformation of the reinforced zone.

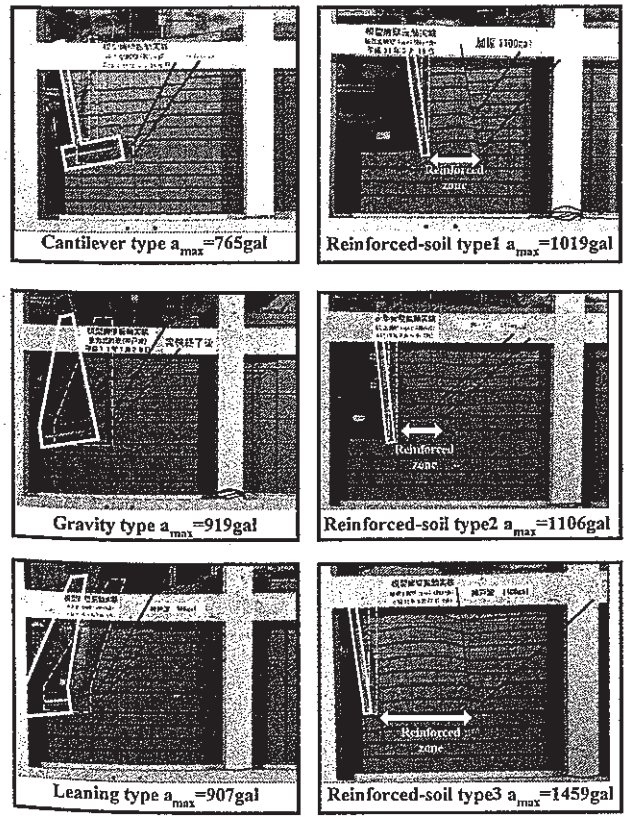

Figure 5. Residual displacement of the wall.

This behavior suggests that the horizontally placed short reinforcement layers cannot effectively resist such simple shear deformation of the reinforced backfill. This simple shear deformation of the reinforced backfill should be considered to evaluate the residual displacement of the wall.

Figure 6 shows the locations of failure plane and the reinforcements for reinforced-soil RW type 2. The arrows indicate the end of longer reinforcement at the moment when the failure planes were formed. The two failure planes were formed almost simultaneously. The upper one developed from the back of the reinforced zone towards just beside the end of the extended reinforcement (45cm), stopping somewhere below the longest reinforcement. On the other hand, the lower failure plane was formed just beside the end of the longest reinforcement (80cm) and reached the surface of the backfill. This demonstrates that the reinforcement resisted against the formation of the failure plane, and the location of the failure plane was strongly governed by the existence of the extended reinforcement. Accordingly, large tensile force was mobilized in the extended reinforcements which will be discussed later.

3.2 *Residual displacement of wall*

Figure 7 shows relationships between the seismic coefficient k_h and the horizontal displacement d_{top} at

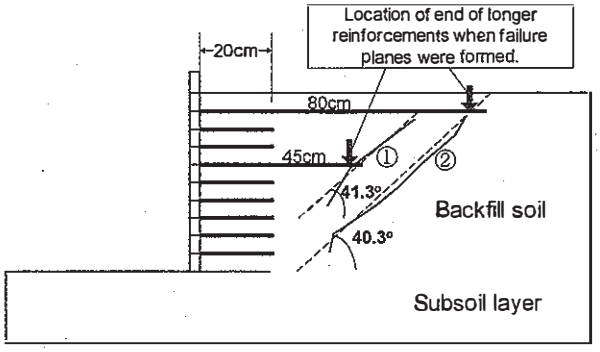

Figure 6. Comparison of locations of failure planes and longer reinforcement layers for reinforced-soil retaining wall type 2.

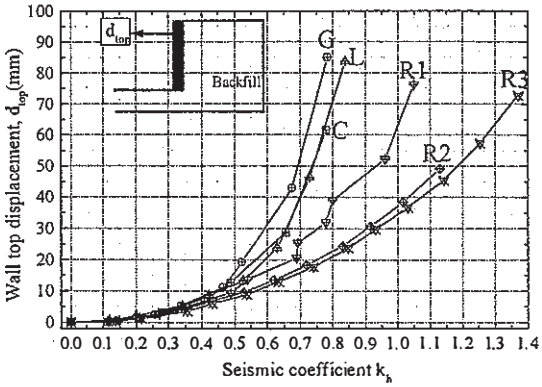

Figure 7. Accumulation of residual horizontal displacement near the top of the wall.

the end of each shaking step which was measured at a distance of 5cm below the top of the wall. The seismic coefficient k_h was defined as $k_h=a_{max}/g$, where a_{max} is the maximum base acceleration at the active state (i.e., when the inertia force was oriented towards the active direction) for each shaking step, and g is the gravitational acceleration. In the early steps of irregular shaking tests up to k_h value of about 0.5, the d_{top} value accumulated in a similar manner among different types of RWs. On the other hand, when the k_h value exceeded about 0.5, the rate of increase in the d_{top} value was larger for the three conventional type RWs than for the reinforced-soil RWs. Further, though the total length of reinforcement of type2 was 80% as much as that of type 3, the seismic stability of them was on the same level. Such different extents of ductility in each type of RW agree with the damage observed after Hyogoken-Nanbu earthquake. This is caused by the different resistance mechanism against the external forces acting on the wall such as inertia force and seismic earth pressure. The details will be discussed in the next two sections.

3.3 *Reaction force from subsoil*

The conventional type RWs resist against the overturning by the reaction force from subsoil. Figure 8 shows the time history of normal stress of the reaction force which includes initial values measured before starting shaking for Gravity type RW. The reaction force was measured by four loadcells at the bottom of base footing. When the inertia force was oriented towards the active direction (Point A), the normal force increased at the toe of the base footing, and decreased at the heel in contrast. This experiment clearly revealed that the wall was rotating around the center of the footing, causing stress concentration at the toe of the base footing.

Figure 9 shows the relationship between the reaction force from subsoil and the horizontal displacement of the wall d_{top}. Figure 10 shows the relationship between the resultant normal force from subsoil and relative location of its application for gravity type retaining wall. Each experimental data was taken when the inertia force towards the active direction was maximized in each shaking step. In the early shaking steps, the normal stress measured at the toe of the base footing increased rapidly (①~⑥ in Figure 9). At this moment, the application point of the resultant force gradually moved toward the toe

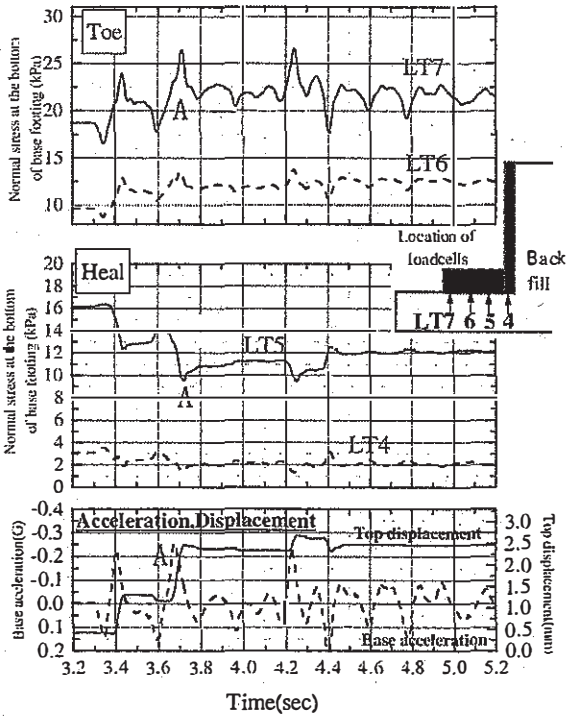

Figure 8. Time history of normal pressure at the bottom of base footing for gravity type retaining wall.

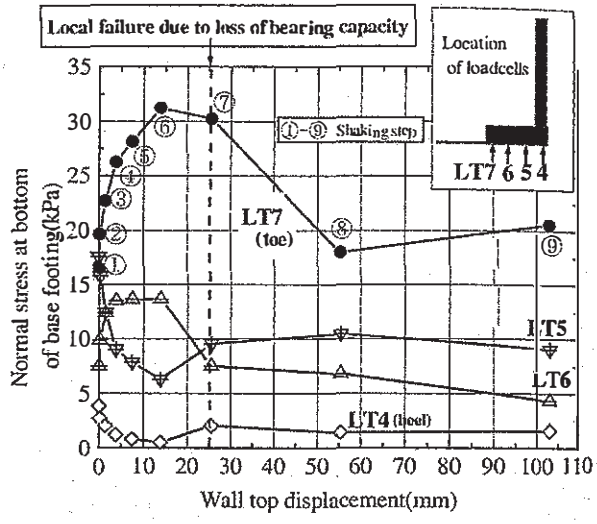

Figure 9. Measured reactions from subsoil for gravity type retaining wall.

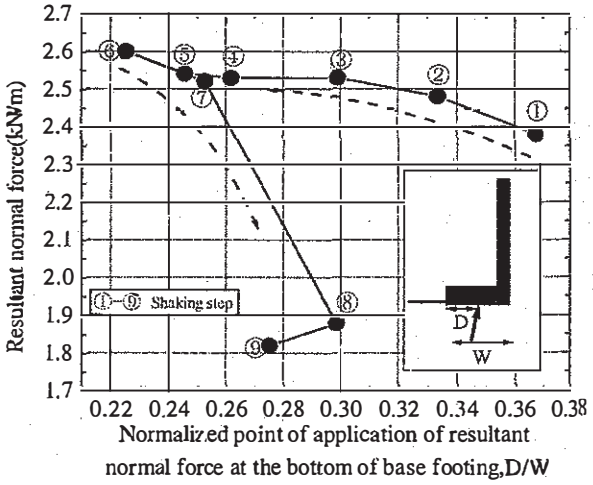

Figure 10. Relationship between resultant normal reaction force from subsoil and relative location of its application.

of the base footing, accompanied with only a slight increase in the amount of the resultant force (①~⑥ in Figure 10). After attaining the peak state, the d_{top} value suddenly increased due to loss of bearing capacity near the toe of the base footing (⑦~⑨ in Figure 9). At this moment, the resultant force decreased suddenly, and its application point moved back toward the heel of the base footing (⑦~⑨ in Figure 10). This behavior caused large decrease in the resisting moment against overturning, which led to the low ductility of conventional type RWs.

3.4 *Tensile force in reinforcement layer*

As mentioned before on Figure 7, the rate of accumulation of the d_{top} value did not increase rapidly for three types of reinforced-soil RWs in irregular shaking tests. The Reinforced-soil RWs resist against the overturning moment by the tensile force in the reinforcements in each layer. Figure 11 shows the time history of tensile force in each reinforcements which were measured at a horizontal distance of 2.5 cm from the facing in the uppermost, middle-height and lowest layers. All tensile forces increased simultaneously to resist against the overturning when the inertia force was oriented towards the active direction (Point A in Figure 11).

Figure 12 shows the relationship between the tensile force and the horizontal displacement of the wall d_{top}. The tensile force data was measured when the inertia force towards the active direction was maximized in each shaking step. For all types of reinforced-soil RWs, the tensile force increased with the d_{top} value, not showing such a sudden drop as observed in the reactions from subsoil for gravity type RW (Figure 9). This may explain the ductile behavior of reinforced-soil RWs.

It can be also seen from Figure 12 that the tensile force in the uppermost layer was largest for reinforced-soil type 2 with longest reinforcement, while it was smallest for reinforced-soil type 1 with shortest reinforcement. In particular, the former value increased even when the d_{top} value was relatively small, while the latter value increased only after the d_{top} value exceeded about 20 mm. These different behaviors may suggest that extension of upper reinforcement layer, such as the case with reinforced-soil type 2, effectively mobilizes the tensile force in the extended reinforcement.

Figures 13a,b and c show the horizontal distribution of tensile force in each reinforcement. As the facing was rigid, almost all the tensile forces were maximized at the nearest point from the facing. For the reinforced-soil RW type 2, however, the tensile force of the uppermost reinforcement (80cm) was largest at a point near of its tip. Such different degree of mobilization of tensile force may be linked to the different locations of these reinforcements relative to the failure planes as typically shown in Figure 6. That is, the tensile force in the uppermost reinforcement for the reinforced-soil RW type 2 was largely mobilized to resist against the formation of the failure plane No.1 (Figure 6) which would have otherwise reached the surface of the backfill.

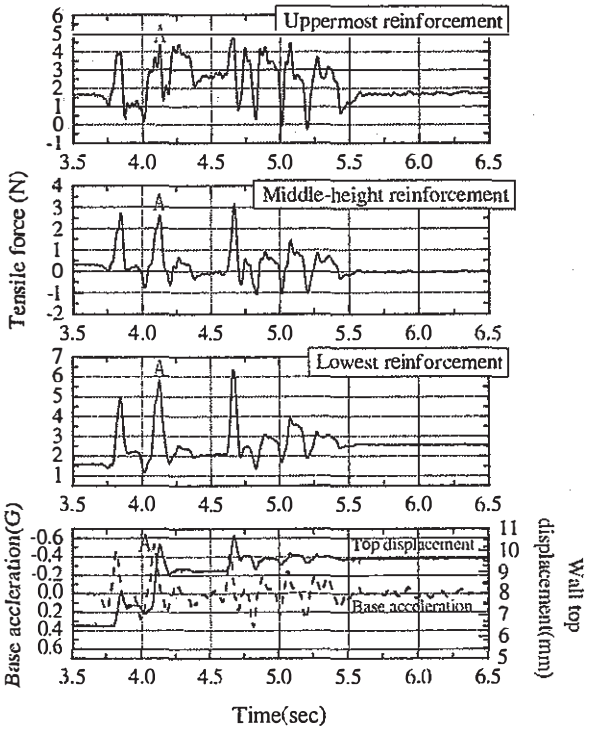

Figure 11. Time history of tensile force in reinforcement for reinforced-soil RW type 2.

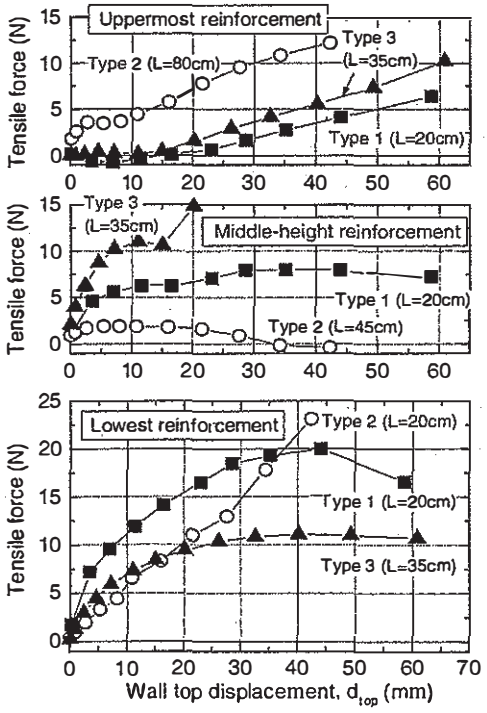

Figure 12. Tensile forces in reinforcement layers measured at a distance of 2.5cm from facing of reinforced-soil RWs.

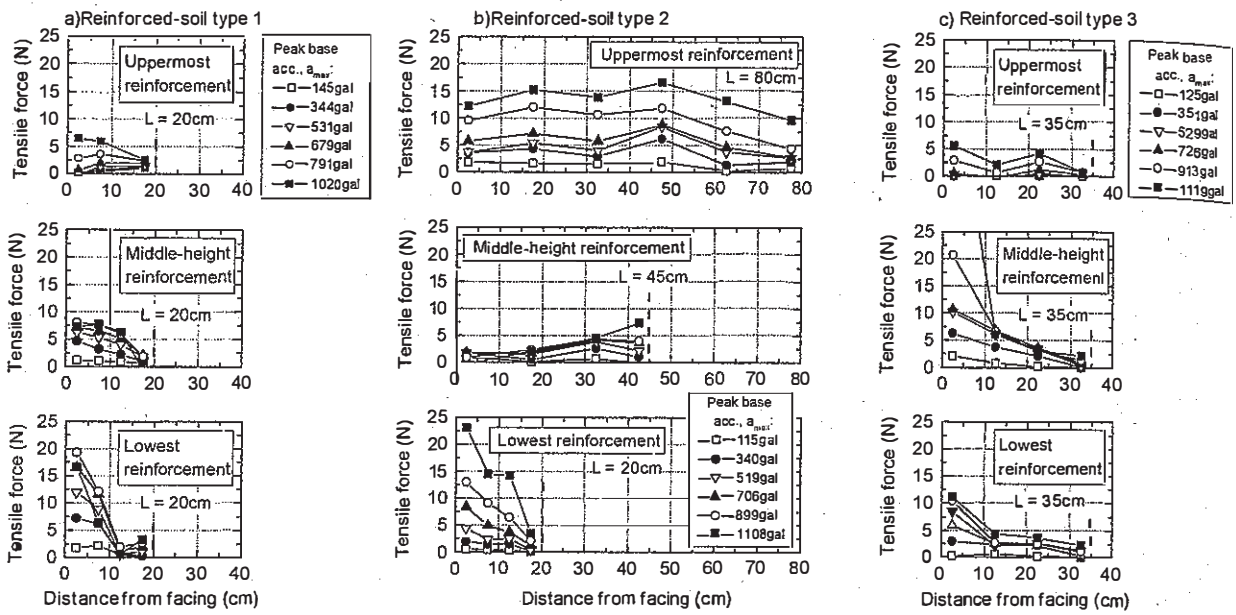

Figure 13. Horizontal distribution of tensile forces in reinforcement layers for reinforced-soil retaining walls a) type 1, b) type 2 and c) type 3.

4 CONCLUSION

Shaking table tests in 1-G field were carried out, and the following conclusions were drawn.

1. At high seismic loads, reinforced-soil type RWs showed more ductile behavior than conventional (cantilever, gravity and leaning) type RWs. When the model walls started to tilt, concentration of subsoil reactions at the toe of conventional type RWs resulted into local failure due to loss of bearing capacity. On the other hand, under similar conditions, tensile force in the reinforcement of the reinforced-soil RWs could be mobilized effectively to resist against the wall movement.
2. It was demonstrated that by extending several upper reinforcements, the seismic stability of reinforced-soil walls could be improved effectively. This is because the tensile force in the extended reinforcement was largely mobilized to resist against the formation of the failure plane.

REFERENCES

Tatsuoka, F., Tateyama, M. & Koseki, J. 1996. Performance of Soil Retaining Walls for Railway Embankments. *Soils and Foundations*, Special Issue of Soils and Foundations on Geotechnical Aspects of the January 17 1995 Hyogoken-Nanbu Earthquake: 311-324.

Koseki, J., Munaf, Y., Tatsuoka, F., Tateyama, M., Kojima, K. & Sato, T. 1998. Shaking Table and Tilt Table Tests of Geosynthetic-Reinforced Soil and Conventional Retaining Wall, *Geosynthetics International*, Vol. 5, Nos. 1-2 :73-96.